Electronic Supplementary Material (ESI) for Journal of Materials Chemistry B

Electronic Supplementary Information

A new light-scattering sensor for screening G-quadruplex stabilizers based on DNA folding-mediated assembly of gold nanoparticles

Da-Qian Feng,[a]‡ Guoliang Liu,[a]‡ Wenjie Zheng,[a] Tianfeng Chen[a] and Dan Li*[b]

[a] Department of Chemistry, College of Life Science and Technology, Jinan University, Guangzhou 510632, China

[b] Department of Chemistry, Shantou University, Guangdong, 515063, China

*E-mail: dli@stu.edu.cn

Experimental section

Materials and Physical measurements

All starting materials and solvents were commercially available and used as received without further purification. Infrared spectra were obtained in KBr disks on a Nicolet Avatar 360 FTIR spectrometer in the range 4000–400 cm^{-1}. Elemental analyses of C, H and N were determined with a Perkin-Elmer 2400C elemental analyzer. ^1H NMR spectra were recorded on a Bruker AVANCE400 spectrometer and referenced to TMS. ESI-MS analyses were carried out using an ABI4000 Q TRAP liquid chromatographymass spectrometer. UV-vis measurements were performed using Agilent 8453 UV-vis spectrophotometer (Agilent Technologies Co. Ltd., USA).

Synthesis of ligands

4′-(4-Methylthiophenyl)-2,2′:6′,2″-terpyridine (L1). 2-Acetylpyridine (7.26 g, 60 mmol) was added into a solution of 4-methylthiobenzaldehyde (4.57 g, 30 mmol) in ethanol (150 mL). Then Solid NaOH (2.58 g, 62 mmol) and $NH_3•H_2O$ (90 mL, 29.3%, 75 mmol) were successively added to the mixed solution. The solution was stirred at room temperature for 6 h. The pale yellow solid was precipitated from the solution, collected and recrystallized in ethanol to yield **L1**.[1] Yield: 3.76 g (35%, 10.6 mmol). m.p. 173 °C. Anal. Calcd for $C_{22}H_{17}N_3S$: C, 74.34%; H, 4.82%; N, 11.82%. Found: C, 74.38%; H, 4.85%; N, 11.84%. ^1H NMR (400 MHz, $CDCl_3$): δ = 8.738 (d, 2H, J = 5.02 Hz, 6,6″ H), 8.723 (s, 2H, 3′,5′ H), 8.662(d, 2H, J = 8.22 Hz, 3,3″ H), 7.866(m, 4H, 4,4″ H), 7.365(m, 4H, 5,5″ H), 2.554 (s, 3H, CH_3). ESI-MS: m/z 356 [$M+H^+$]. IR (KBr, cm^{-1}): 3051 w, 2918 w, 1583 s, 1561 m, 1495 m, 1387 m, 1093 w, 817 m, 789 m.

4′-(4-Isopropylphenyl)-2,2′:6′,2″-terpyridine (L2). 4′-(4-Isopropylphenyl)-2,2′:6′,2″-terpyridine was prepared analogously to **L1**, but with 4-isopropylbenzaldehyde (4.44 g, 30 mmol) in place of 4-methylthiobenzaldehyde. Yield: 3.47 g (33%, 9.9 mmol). Anal. Calcd for $C_{24}H_{21}N_3$: C, 82.02%; H, 6.02%; N, 11.96%. Found: C, 82.08%; H,

6.06%; N, 11.86%. ^{1}H NMR (400 MHz, DMSO): δ = 8.79 (d, 2H, J = 7.26 Hz, 6,6″ H), 8.53 (s, 2H, 3′,5′ H), 8.462(d, 2H, J = 8.10 Hz, 3,3″ H), 7.78(m, 4H, 4,4″ H), 7.37(m, 4H, 5,5″ H), 3.13(m, 1H), 2.01 (s, 6H, CH_3). ESI-MS: m/z 351.21 [M^+]. IR (KBr, cm^{-1}): 3023 w, 2959 m, 2922 w, 1593 s, 1559 m, 1485 m, 1397 m, 1093 w, 993 m, 821 m.

4′-(4-Dimethylaminophenyl)-2,2′:6′,2″-terpyridine (L3). 4′-(4-Dimethylaminophenyl)-2,2′:6′,2″-terpyridine was prepared analogously to **L1**, but with 4-dimethyl-aminobenzaldehyde (4.47 g, 30 mmol) in place of 4-methylthiobenzaldehyde. Yield: 3.91 g (37%, 11.1 mmol). m.p. 206 °C. Anal. Calcd for $C_{23}H_{20}N_4$: C, 78.38%; H, 5.72%; N, 15.90%. Found: C, 78.32%; H, 5.70%; N, 15.98%. ^{1}H NMR (400 MHz, DMSO): δ = 8.79 (s, 2H), 8.723 (m, 4H), 7.99(t, 2H, J = 2.02 Hz), 7.84(d, 2H, J = 9.2 Hz), 7.465(t, 2H, J = 1.2 Hz), 6.94(d, 2H, J = 2.01 Hz), 3.06 (s, 6H, $N(CH_3)_2$). ESI-MS: m/z 352.3 [M^+]. IR (KBr, cm^{-1}): 3021 w, 1591 s, 1588 s, 1540 m, 1387 m, 1355 w, 1210 m, 1068 w, 949 m, 816 s.

4′-(4-Ethylphenyl)-2,2′:6′,2″-terpyridine (L4). 4′-(4-Ethylphenyl)-2,2′:6′,2″-terpyridine was prepared analogously to **L1**, but with 4-ethylbenzaldehyde (4.02 g, 30 mmol) in place of 4-methylthiobenzaldehyde. Yield: 4.15 g (41%, 12.3 mmol). Anal. Calcd for $C_{23}H_{19}N_3$: C, 81.87%; H, 5.68%; N, 12.45%. Found: C, 81.98%; H, 5.74%; N, 12.28%. ^{1}H NMR (400 MHz, DMSO): δ = 8.87 (d, 2H, J = 7.68 Hz, 6,6″ H), 8.78 (s, 2H, 3′,5′ H), 8.50(d, 2H, J = 9.01 Hz, 3,3″ H), 7.66(m, 4H, 4,4″ H), 7.45(m, 4H, 5,5″ H), 2.59(m, 2H), 1.25(m, 3H, CH_3). ESI-MS: m/z 337.1 [M^+]. IR (KBr, cm^{-1}): 3032 w, 2974 w, 1593 s, 1539 m, 1495 m, 1393 m, 1093 w, 997 m, 789 m.

Synthesis of complexes

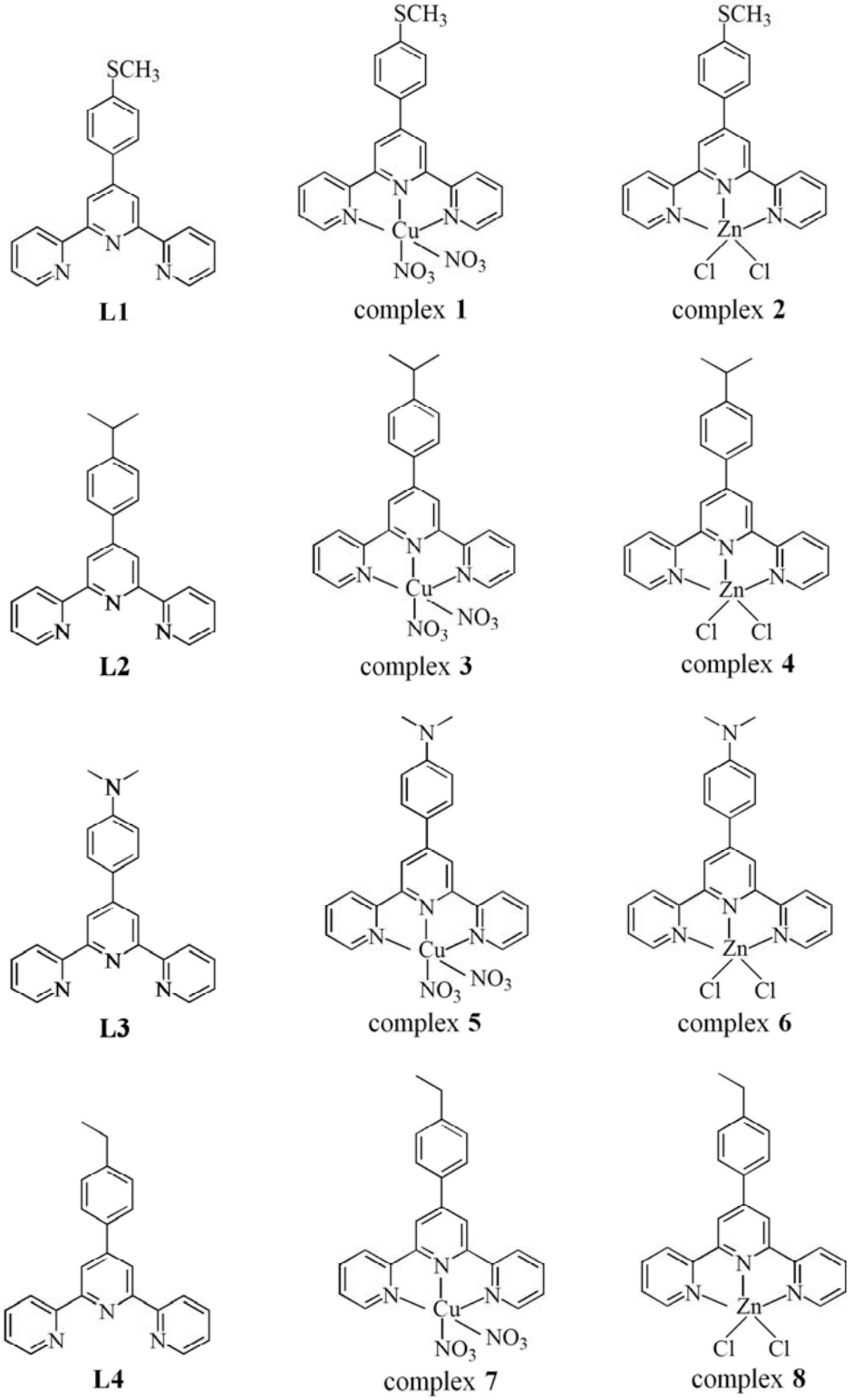

Figure S1. Structure of terpyridines **L1**–**L4** and their corresponding metal complexes

1–8.

[Cu(L1)(NO$_3$)$_2$] (1). A blue solution of Cu(NO$_3$)$_2$ (0.0225 g, 0.093 mmol, 1.0 equiv.) in 2 mL of ethanol was slowly added to a colorless solution of **L1** (0.033 g, 0.093 mmol, 1.0 equiv.) in 4 mL of dichloromethane. Then the mixed solution was stirred for 3 hours. The resulting precipitate was filtered, then washed with water, ethanol, and dried with diethyl ether. [Cu(**L1**)(NO$_3$)$_2$] is obtained as green solid (Yield: 0.0204g, 49%). Anal. Calcd for $C_{22}H_{17}CuN_5O_6S$: C, 48.66%; H, 3.16%; N, 12.90%. Found: C, 48.70%; H, 3.18%; N, 12.92%. ^{1}H NMR (400 MHz, DMSO): δ = 9.091 (d, 2H, J = 5.15 Hz, 6,6″ H), 8.974 (s, 2H, 3′,5′ H), 8.849(d, 2H, J = 8.34 Hz, 3,3″ H), 8.29-8.01 (m, 4H, 4,4″ H), 7.88-7.54(m, 4H, 5,5″ H), 2.611 (s, 3H, CH$_3$). ESI-MS: m/z 481 [Cu(**L1**)(NO$_3$)]$^+$. IR (KBr, cm^{-1}): 3063 w, 2918 w, 1592 s, 1478 m, 1383m, 1099 m, 1020w, 830 m, 792 m. UV-vis data: λ_{max} (nm): 254, 265, 275, 285, 345.

[Zn(L1)Cl$_2$] (2). To a solution of **L1** (0.033 g, 0.093 mmol, 1.0 equiv.) in 4 mL of dichloromethane is added drop wise a solution of ZnCl$_2$ (0.0127g, 0.093mmol, 1.0equiv.) in 2 mL of ethanol. Then the mixed solution was stirred for 3 hours. The resulting pale yellow precipitate was filtered, then washed with water, ethanol, and dried with diethyl ether. [Zn(**L1**)Cl$_2$] is obtained as white solid (Yield: 0.0219 g, 48%). Anal. Calcd for $C_{22}H_{17}ZnN_3Cl_2S$: C, 53.73%; H, 3.48%; N, 8.54%. Found: C, 53.70%; H, 3.52%; N, 8.58%. ^{1}H NMR (400 MHz, DMSO): δ = 9.01 (d, 2H, J = 5.08 Hz, 6,6″ H), 8.87 (s, 2H, 3′,5′ H), 8.6 (d, 2H, J = 8.26 Hz, 3,3″ H), 8.19 (m, 4H, 4,4″ H), 7.88-7.54 (m, 4H, 5,5″ H), 2.5 (s, 3H, CH$_3$). ESI-MS: m/z 454.41 [Zn(**L1**)Cl]$^+$. IR (KBr, cm^{-1}): 3062 w, 2920 w, 1591 s, 1475 m, 1381 m, 1098 m, 1019 w, 830 m, 797

m. UV-vis data: λ_{max} (nm): 247, 263, 279, 337.

[Cu(L2)(NO$_3$)$_2$] (3). The procedure for preparing **3** was identical to that for preparing **1**, expect **L1** was replaced with **L2** (0.0326 g, 0.093 mmol, 1.0 equiv.). [Cu(**L2**)(NO$_3$)$_2$] is obtained as blue solid (Yield: 0.0290g, 58%). Anal. Calcd for $C_{24}H_{21}CuN_5O_6$: C, 53.48%; H, 3.93%; N, 12.99%. Found: C, 53.51%; H, 3.98%; N, 12.87%. ^{1}H NMR (400 MHz, DMSO): δ = 9.0 (d, 2H, J = 7.22 Hz, 6,6″ H), 8.79 (s, 2H, 3′,5′ H), 8.6 (d, 2H, J = 8.36 Hz, 3,3″ H), 7.8 (m, 4H, 4,4″ H), 7.35 (m, 4H, 5,5″ H), 3.3 (m, 1H, CH), 2.51 (d, 6H, CH$_3$). ESI-MS: m/z 476 [Cu(**L2**)(NO$_3$)]$^+$. IR (KBr, cm^{-1}): 3034 w, 2958 m, 2917 w, 1591 s, 1558 m, 1479 m, 1397 m, 1093 w, 997 m, 820 m.

[Zn(L2)Cl$_2$] (4). The procedure for preparing **4** was identical to that for preparing **2**, expect **L1** was replaced with **L2** (0.0326 g, 0.093 mmol, 1.0 equiv.). [Zn(**L2**)Cl$_2$] is obtained as white solid (Yield: 0.0212 g, 47%). Anal. Calcd for $C_{24}H_{21}ZnN_3Cl_2$: C, 59.10%; H, 4.34%; N, 8.62%. Found: C, 59.15%; H, 4.38%; N, 8.59%. ^{1}H NMR (400 MHz, DMSO): δ = 9.02 (d, 2H, J = 7.24 Hz, 6,6″ H), 8.80 (s, 2H, 3′,5′ H), 8.66 (d, 2H, J = 8.27 Hz, 3,3″ H), 7.9 (m, 4H, 4,4″ H), 7.36 (m, 4H, 5,5″ H), 3.25 (m, 1H, CH), 2.55 (d, 6H, CH$_3$). ESI-MS: m/z 450 [Zn(**L2**)Cl]$^+$. IR (KBr, cm^{-1}): 3449 w, 2958 w, 1595 s, 1557 m, 1516 s, 1497 m, 1396 m, 1098 m, 1019 w, 993 w, 830 m, 797 m.

[Cu(L3)(NO$_3$)$_2$] (5). The procedure for preparing **5** was identical to that for preparing **1**, expect **L1** was replaced with **L3** (0.0326 g, 0.093 mmol, 1.0 equiv.). [Cu(**L3**)(NO$_3$)$_2$] is obtained as blue solid (Yield: 0.0231g, 46%). Anal. Calcd for $C_{23}H_{20}CuN_6O_6$: C, 51.16%; H, 3.73%; N, 15.56%. Found: C, 51.13%; H, 3.70%; N,

15.72%. ^{1}H NMR (400 MHz, DMSO): δ = 9.0 (s, 2H), 8.77 (m, 4H), 8.0(t, 2H, J = 2.10 Hz), 7.84(d, 2H, J = 9.10 H*z*), 7.45(t, 2H, J = 1.10 Hz), 6.99(d, 2H, J = 2.02 Hz), 3.15 (s, 6H, N(CH_3)$_2$). ESI-MS: *m*/*z* 477.11 [M^+]. IR (KBr, cm^{-1}): 3031 w, 1590 s, 1589 s, 1535 m, 1389 m, 1367 w, 1211 m, 1067 w, 947 m, 817 s.

[Zn(L3)Cl$_2$] (6). The procedure for preparing **6** was identical to that for preparing **2**, expect **L1** was replaced with **L3** (0.0326 g, 0.093 mmol, 1.0 equiv.). [Zn(**L3**)Cl_2] is obtained as white solid (Yield: 0.0236 g, 52%). Anal. Calcd for $C_{23}H_{20}ZnN_4Cl_2$: C, 56.52%; H, 4.12%; N, 11.46%. Found: C, 56.53%; H, 4.10%; N, 11.48%. ^{1}H NMR (400 MHz, DMSO): δ = 9.02 (s, 2H), 8.76 (m, 4H), 8.01(t, 2H, J = 2.06 Hz), 7.85(d, 2H, J = 9.20 Hz), 7.47(t, 2H, J = 1.18 Hz), 6.81(d, 2H, J = 2.03 Hz), 3.17 (s, 6H, N(CH_3)$_2$). ESI-MS: *m*/*z* 451.13 [Zn(**L3**)Cl]$^+$. IR (KBr, cm^{-1}): 3032 w, 1593 s, 1540 m, 1426 m, 1393 m, 1213 m, 1062 w, 997 m, 817 m. UV-vis data: λ_{max} (nm): 290, 350, 418, 438.

[Cu(L4)(NO$_3$)$_2$] (7). The procedure for preparing **7** was identical to that for preparing **1**, expect **L1** was replaced with **L4** (0.0326 g, 0.093 mmol, 1.0 equiv.). [Cu(**L4**)(NO_3)$_2$] is obtained as blue solid (Yield: 0.0268 g, 55%). Anal. Calcd for $C_{23}H_{19}CuN_5O_6$: C, 52.62%; H, 3.65%; N, 13.34%. Found: C, 52.67%; H, 3.69%; N, 12.29%. ^{1}H NMR (400 MHz, DMSO): δ = 9.02 (d, 2H, J = 7.70 Hz, 6,6″ H), 8.87 (s, 2H), 8.66(d, 2H, J = 9.02 Hz, 3,3″ H), 7.7(m, 4H), 7.46(m, 4H), 2.55(m, 2H), 1.25(m, 3H, CH_3). ESI-MS: *m*/*z* 462 [Cu(**L4**)(NO_3)]$^+$. IR (KBr, cm^{-1}): 3034 w, 2975 w, 1591 s, 1538 m, 1488 m, 1397 m, 1087 w, 989 m, 788 m.

[Zn(L4)Cl$_2$] (8). The procedure for preparing **8** was identical to that for preparing **2**,

expect **L1** was replaced with **L4** (0.0326 g, 0.093 mmol, 1.0 equiv.). [Zn(**L4**)Cl_2] is obtained as white solid (Yield: 0.0229 g, 53%). Anal. Calcd for $C_{23}H_{19}ZnN_3Cl_2$: C, 58.32%; H, 4.04%; N, 8.87%. Found: C, 58.37%; H, 4.06%; N, 8.84%. ^{1}H NMR (400 MHz, DMSO): δ = 9.01 (d, 2H, J = 7.62 Hz, 6,6″ H), 8.89 (s, 2H), 8.67(d, 2H, J = 8.98 Hz, 3,3″ H), 7.72(m, 4H), 7.45(m, 4H), 2.57(m, 2H), 1.253(m, 3H, CH_3). ESI-MS: m/z 436 [Zn(**L4**)Cl]$^+$. IR (KBr, cm^{-1}): 3033 w, 2978 w, 1592 s, 1539 m, 1491 m, 1398 m, 1089 w, 987 m, 791 m.

Table S1. The oligonulceotides used are listed in the 5’ to 3’ direction.

Name	Sequences (5’-3’)	DNA size (bp)
G-rich unit ssDNA	HS-$(CH_2)_6$-T_{10}-TTAGGG	16
Space ssDNA	HS-$(CH_2)_6$- T_{10}-TTA	13
Human telomeric G-rich ssDNA	TAGGG$(TTAGGG)_3$	23

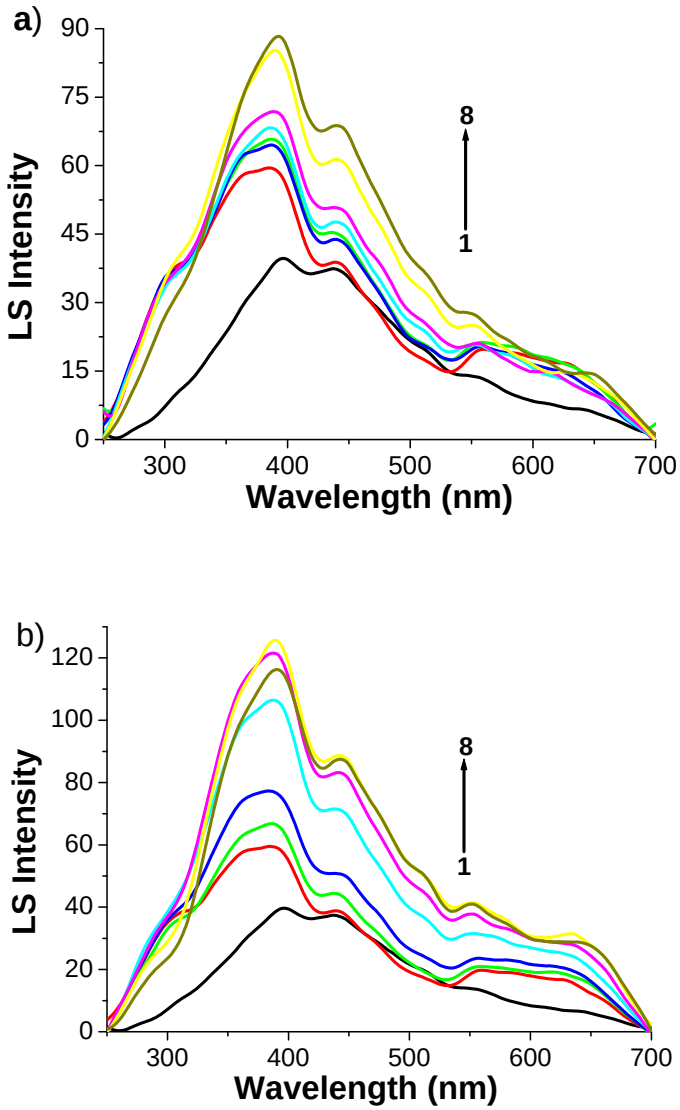

Figure S2. The light-scattering spectra of gold nanoparticles functionalized human telomeric G-rich ssDNA (G-rich ssDNA-S-Au NPs) in the presence of increasing K^+ (a) or Na^+ (b) concentrations. Conditions: a): 1, Blank; 2, Au NPs functionalized G-rich ssDNA; 3-8: 2 + K^+ (mM): 2.5, 5, 7.5, 10, 12.5, 15. b): 1, Blank; 2, Au NPs functionalized G-rich ssDNA; 3-8: Au NPs + Na^+ (mM): 5, 10, 15, 20, 25, 30.

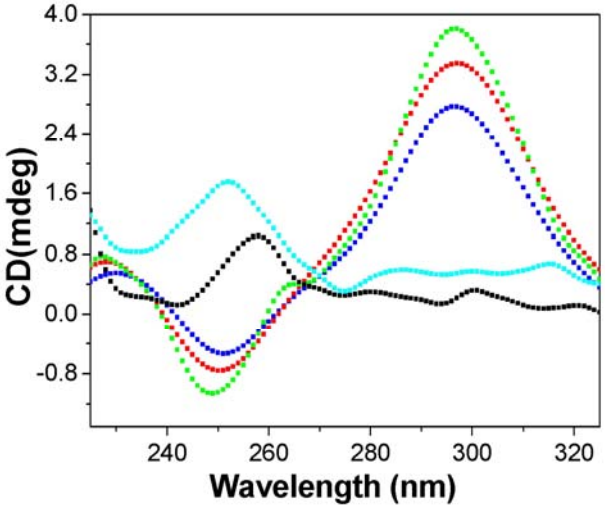

Figure S3. CD Spectra of G-rich single-stranded oligonucleotide (TAGGG(TTAGGG)$_3$) (4.0 μM) in the absence (black) and presence of ligand (**L1**) (5.0 μM, cyan) or increasing concentration of metal complex **1** (μM): 4.0 (blue), 8.0 (red), 12.0 (green) in Tris/HCl buffer (10 mM Tris, pH 7.4).

The metal-terpyridine complex-induced formation of the human telomeric G-quadruplex structure was monitored using Circular Dichroism (CD) spectroscopy. Without adding any metal cations, CD spectrum of the human telomeric DNA sequence (TAGGG(TTAGGG)$_3$) exhibited a positive peak at 256 nm and a negative one at 235 nm, which suggests that human telomeric DNA exists as a single-stranded structure at the conditions. However, upon the addition of complex **1**, a dramatic change in CD spectrum was observed. The intensity of the positive CD band at 256 nm decreased gradually from positive to negative with continually blue shift. Meanwhile, a remarkable increase of the CD band at 295 nm and an emergence of a shoulder peak at 265 nm were observed to appear (Figure S3). The band centred at

about 295 nm increased dramatically along with an increase of the concentration of complex **1**. These situations reveal the formation of G-quadruplex between nanoparticles. Additionally, it does not appear the characteristic peak of G-quadruplex after adding the ligand (**L1**) into $TAGGG(TTAGGG)_3$. Meanwhile, Complex **1** can facilitate and stabilize G-quadruplex conformation. Therefore, it can be concluded that the assembly of Au NPs-based biosensor are due to the fact that G-quadruplex is formed between nanoparticles.

Figure S4. Color response of DNAzyme system in the absence (left, colorless) or presence (right, blue-green) of complex **1**.

It is well known that G-quadruplex DNA which can be effectively formed in the presence of a stabilizer has the ability to bind with hemin to form peroxidase-like DNAzyme. It is proven that in the presence of the DNAzyme, H_2O_2-mediated oxidation of TMB (3,3',5,5'-tetramethylbenzidine) could be sharply accelerated and the color change is very sensitive and easy to identify. The design is based on this principle. As shown in Fig. S4, in the presence of complex **1**, human telomeric TAGGG(TTAGGG)$_3$ can also fold into G-quadruplex, forming G-quadruplex DNAzyme after the addition of hemin, which catalyzes the H_2O_2-mediated oxidation of colorless TMB (3,3',5,5'-tetramethylbenzidine) to the blue-green product.

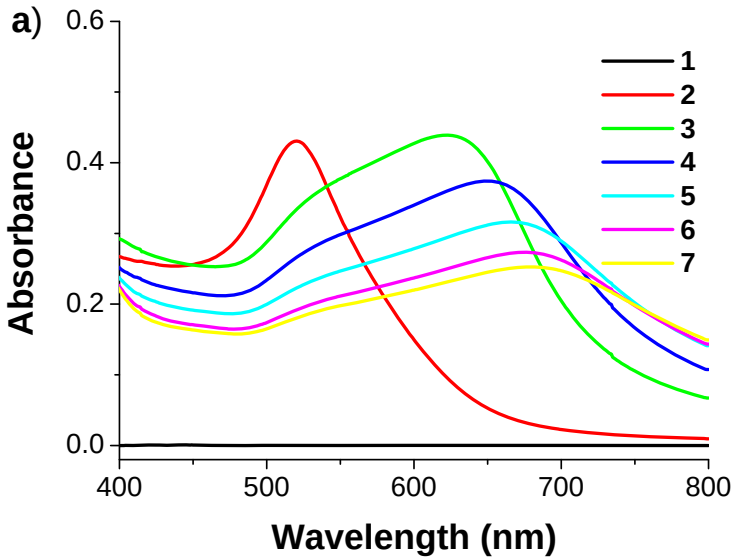

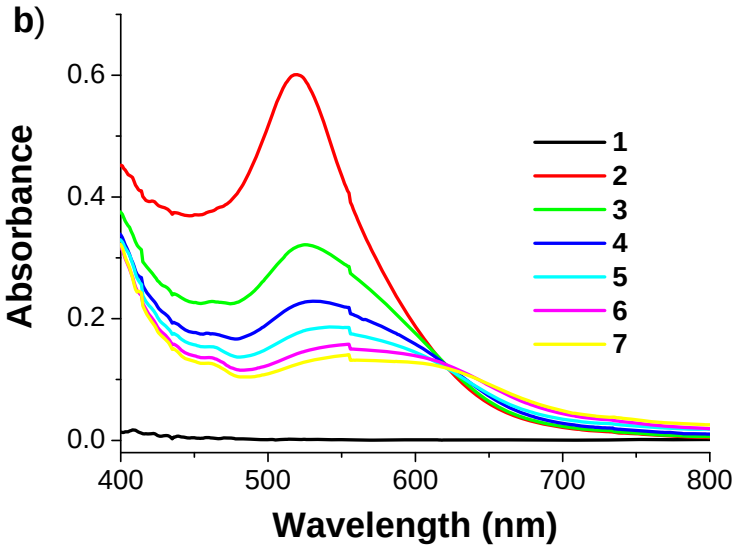

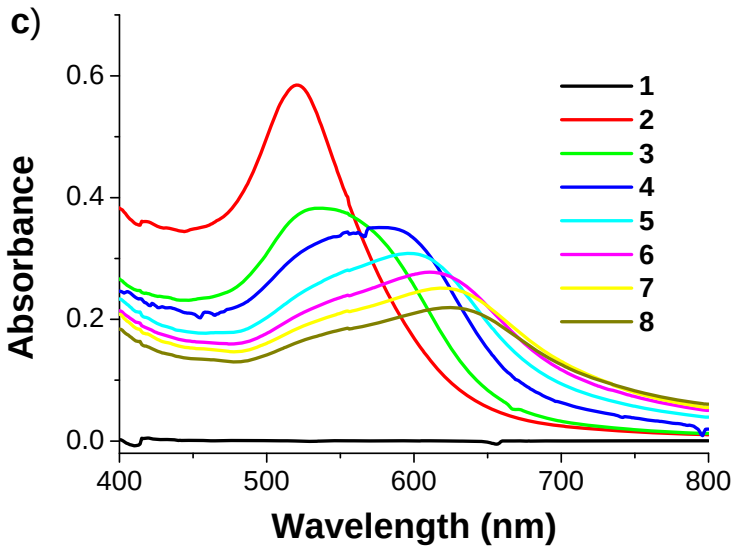

Figure S5. UV-vis spectra of gold nanoparticles functionalized with G-rich unit ssDNA in the absence and presence of increasing concentration of complex **2** (a), or K^+ (b), or Na^+ (c) in Tris/HCl buffer (10 mM Tris, pH 7.4). Conditions: a) 1, the buffer solution (blank); 2, the solution of Au NPs functionalized with G-rich unit ssDNA; 3-7, 2 + complex **2** (μM): 5, 10, 15, 20, 25; b) 1, the buffer solution (blank); 2, the solution of Au NPs functionalized with G-rich unit ssDNA; 3-7, 2 + K^+ (M): 0.005, 0.01, 0.015, 0.02, 0.025; c) 1, the buffer solution (blank); 2, the solution of Au NPs functionalized with G-rich unit ssDNA; 3-8, 2 + Na^+ (M): 0.01, 0.02, 0.03, 0.04, 0.05, 0.06.

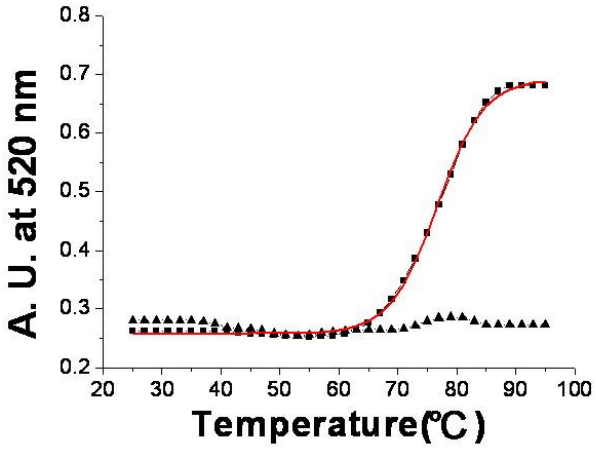

Figure S6. Absorbance melting profiles of G-rich ssDNA (TAGGG(TTAGGG)$_3$)-S-Au NPs aggregates in the absence (triangle) or present (square, T_m = 77 °C) of metal complex **1** (10 μM) in 10 mM Tris-HCl buffer (pH 7.4). Note: the red line is the fitting curve.

Heat up the solution from 25°C to 95°C at a rate of 2°C/min while its extinction is monitored at 520 nm, where the Au NPs-based biosensor exhibit the maximum intensity in the visible region of the spectrum. The T_m is obtained at the maximum of the first derivative of the melting transition.

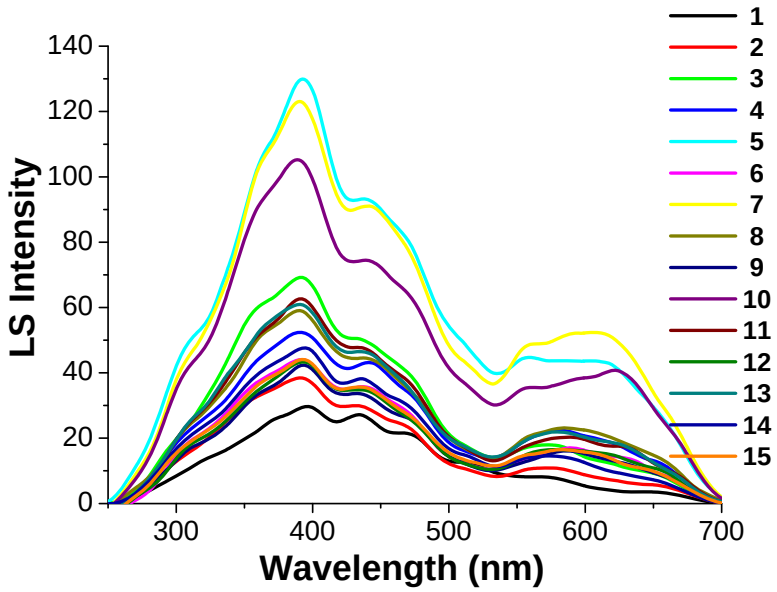

Figure S7. Light scattering (LS) spectra of screening G-quadruplex stabilizers (metal-terpyridine complexes) by Au NPs-based biosensor. Conditions: (1) the buffer solution; (2) the biosensor-Au NPs functionalized G-rich unit ssDNA; (3) **L1** ligand; (4) complex **2**; (5) complex **1**; (6) **L2** ligand; (7) complex **3**; (8) complex **4**; (9) **L3** ligand; (10) complex **5**; (11) complex **6**; (12) **L4** ligand; (13) complex **7**; (14) complex **8**; (15) cisplatin. All complexes (ligands or drugs) were tested at 5 μM.

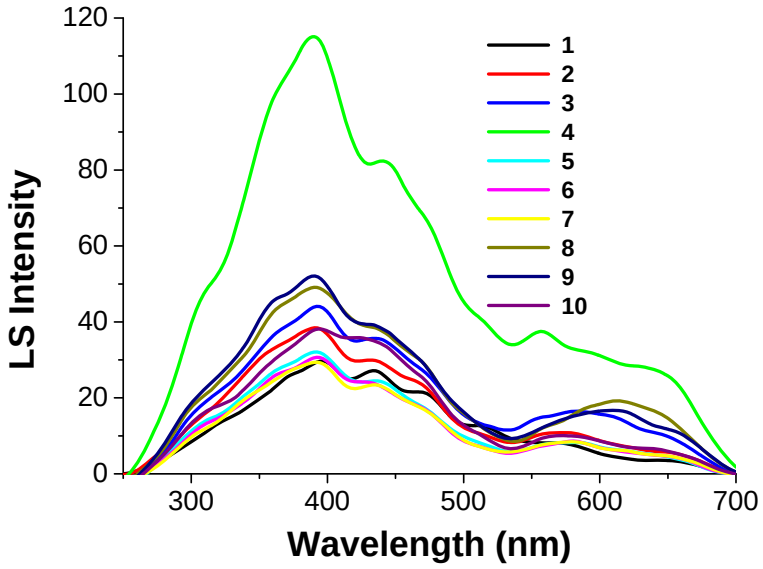

Figure S8. Light scattering (LS) spectra of screening G-quadruplex stabilizers (drugs) by Au NPs-based biosensor. Conditions: (1) the buffer solution; (2) the biosensor-Au NPs functionalized G-rich unit ssDNA; (3) cisplatin; (4) MTX (Mitoxantrone); (5) berberine; (6) acetaminophen; (7) amoxicillin; (8) TO; (9) methyl green; (10) hemin. All drugs were tested at 5 μM.